BASIC SCIENCE

Nanomedicine: Nanotechnology, Biology, and Medicine
16 (2019) 173 – 184

Original Article

nanomedjournal.com

Ultra-small but ultra-effective: Folic acid-targeted gold nanoclusters for enhancement of intracranial glioma tumors' radiation therapy efficacy

Amirhosein Kefayat, MD[a], Fatemeh Ghahremani, PhD[b,*], Hasan Motaghi, PhD[c], Alireza Amouheidari, MD[d]

[a]*Department of Oncology, Cancer Prevention Research Center, Isfahan University of Medical Sciences, Isfahan, Iran*
[b]*Department of Medical Physics and Radiotherapy, Arak University of Medical Sciences, Arak, Iran.*
[c]*Department of Science, Farhangian University, Tehran, Iran*
[d]*Department of Radiation Oncology, Isfahan Milad Hospital, Isfahan, Iran*

Abstract

The aim of the present study is to investigate folic acid and BSA decorated gold nanoclusters (FA-AuNCs) effect on the enhancement of intracranial C6 glioma tumors radiation therapy (RT) efficacy. Inductively coupled plasma optical emission spectrometry (ICP-OES) measurements exhibited about 2.5 times more FA-AuNCs uptake by C6 cancer cells (32.8 ng/10^6 cells) than the normal cells. FA-AuNCs had significantly higher concentration in the brain tumors (8.1 μg/mg) in comparison with surrounding normal brain tissue (4.3 μg/mg). Moreover, FA-AuNCs exhibited dose enhancement factor (DEF) of 1.6. The glioma-bearing rats' survival times were almost doubled at radiation therapy + FA-AuNCs (25.0 ± 1.5 days) in comparison with no-treatment group (12.8 ± 0.7 days). The Ki-67 labeling index was 48.89% ± 9.93 for control, 29.98% ± 8.32 for RT, and 11.53% ± 7.65 for RT + FA-AuNCs. Therefore, FA-AuNCs can be effective radiosensitizers for intracranial glioma tumors RT.

Key words: Gold nanoclusters; Folic acid; Radiosensitizer; Brain tumor; Blood–brain barrier

Glioblastoma multiform (GBM) is the most common malignancy of the glial cells.[1] GBM patients' prognosis is extremely poor with about one-year survival.[2] Although radiation therapy (RT) is the main modality for GBM therapy, clinical and experimental studies have shown considerable treatment failure and unsatisfying outcomes due to GBM radioresistance.[3] Therefore, novel approaches for enhancing the GBM radiation therapy efficacy have received lots of attention.

Use of nanoparticles as radiosensitizer can significantly enhance the radiation therapy efficacy for different tumors.[4] However, there is a big obstacle for efficient delivery of nanoparticles to the intracranial tumors like GBM which is the blood–brain barrier (BBB).[5] This barrier restricts the transfer of systemic injected anticancer agents to intracranial tumors. Crossing the BBB is the first obstacle and nanoparticles should also have the ability to target the cancer cells in the brain tissue.[6]

Gold nanoparticles (GNPs) are an important category among the radiosensitizers with nanostructure, due to their high stability,[7] biocompatibility,[8] high atomic number,[2] and the ability to be synthesized at diverse sizes and characterizations.[9]

Abbreviations: RT, Radiation therapy; FA, Folic acid; BSA, Bovine serum albumin; AuNCs, Gold nanoclusters; BBB, Blood–brain barrier; PBS, Phosphate buffer solution; DEF, Dose enhancement factor; SSD, Surface-surface distance; SSC, Side scatter; ALT, Alanine transaminase; AST, Aspartate transaminase; BUN, Blood urea nitrogen; CREA, Creatinine.

Financial and competing interests' disclosure: This work was supported by the Arak University of Medical Sciences (grant number: 3272), Arak, Iran. The authors declare that they have no other relevant affiliations or financial involvement with any organization or entity with a financial interest or financial conflict with the subject matter or materials discussed in the manuscript apart from those disclosed. No writing assistance was utilized in the production of this manuscript. The authors declare that they have no conflicts of interest.

*Corresponding author at: Arak Uni. of Medical Sciences, Arak, Iran.
E-mail address: F.ghahremani@arakmu.ac.ir (F. Ghahremani).

https://doi.org/10.1016/j.nano.2018.12.007
1549-9634/

Please cite this article as: Kefayat A, et al, Ultra-small but ultra-effective: Folic acid-targeted gold nanoclusters for enhancement of intracranial glioma tumors' radiation therapy efficacy. *Nanomedicine: NBM* 2019;16:173-184, https://doi.org/10.1016/j.nano.2018.12.007

GNPs can be designed to provide desirable functionalities.[10] Appropriate decoration can enhance the internalization of GNPs into the brain through the increase of their interactions with specific molecules which are expressed on the luminal side of BBB endothelial cells.[11] High concentration of GNPs in the cancer cells in comparison with the normal surrounding tissue causes significant deposition of radiation beams' energy at the tumor and consequent cancer cell damage and enhancement of radiation therapy efficacy.[12]

The aim of the present study is to introduce an effective gold nanostructure as a functionalized radiosensitizer for improving the intracranial tumors radiation therapy efficacy. For this purpose, gold nanoclusters with specific characterizations including ultra-small size and smart decoration for BBB transfer and intracranial glioma tumor targeting were designed and synthesized. Subsequently, their efficacy as glioma radiosensitizer was assessed according to tumor targeting efficacy, brain tissue biocompatibility, radiosensitizing effect for inhibition of tumors growth and proliferation and increase of the glioma tumor-bearing rats' survival.

Methods

Folic acid-bovine serum albumin-gold nanoclusters synthesis (FA-AuNCs)

Synthesis of blue-emitting (λ = 450 nm) small gold nanoclusters was done based on previously published studies.[13] Briefly, folic acid was prepared as 5% (m/v) stock solution in sodium carbonate buffer (20 mM, pH 8.5). Folic acid stock solution was added into BSA solution (5 mg/mL) with a molar ratio 800:1 (FA: BSA). NHS and EDC were added to achieve high efficiency of amidation with a molar ratio of 1:1.5:20 (FA: NHS: EDC). Folic acid was attached onto BSA through amidation with amino-groups on BSA (FA-BSA). Subsequently, 5 mL of FA-BSA was added to 5 mL aqueous solution of $HAuCl_4$ (10 mM) under vigorous stirring at 37 °C. Fifty microliters of ascorbic acid (0.35 mg/mL) was added dropwise to trigger the formation of gold nanoclusters (FA-AuNCs). Then the solution pH was adjusted at 9 with NaOH.

FA-AuNCs characterization

A FT-IR spectrophotometer (JASCO, Tokyo, Japan) was employed for characterizing the Fourier transform infrared (FT-IR) spectra of FA-AuNCs. UV–Vis and fluorescence were evaluated by UV-160 and RF-5301PC Spectrofluorometers (Shimadzu, Tokyo, Japan), respectively. In addition, the nanoclusters' size was determined by dynamic light scattering (DLS) technique using Vasco nanoparticle size analyzer (Cordouan Technologies, Pessac, France). The fluorescence quantum yield (QY) of the synthesized nanoclusters was determined using the reference point method by comparing their excitation and emission with fluorescein as a standard fluorescent compound.[14]

Cell culture

C6 (rat glioma) and L929 (normal fibroblast) cell lines were obtained from Pastor Institute of Tehran, Iran. L929 cells were cultured in Roswell Park Memorial Institute medium 1640 (Sigma, CA, USA) with 10% fetal bovine serum (Sigma, CA, USA). The C6 cells were grown in DMEM-F12 containing FBS and horse serum to the final concentration of 2.5% and 15%, respectively.

Cell viability assay

MTT assay was utilized to assess the cytotoxic effect of different concentrations of FA-AuNCs. Moreover, the C6 and L929 cell lines were used as the cancer and normal cells, respectively. 96-well plates were used and each well was seeded with 10^4 cells. The plates were incubated at standard cell culture condition for 24 h. Different concentrations of FA-AuNCs (10, 20, 40, 80,160, and 320 μg/mL) were added to the wells. Each well's final volume reached 200 μL with addition of suitable culture media. The cells' viability was evaluated after 24 h with an MTT assay kit according to the manufacturer's instructions.[15] All samples were performed in triplicate.

Fluorescence microscopy

10^5 C6 cells were seeded at 6-well culture plates and incubated for 24 h. Then, 160 μg/mL FA-AuNCs were added to wells and were incubated for another 24 h. The cells were washed 3 times with phosphate buffered saline (1×, pH 7.4) to remove non-internalized nanoclusters and the FA-AuNCs internalization was estimated by fluorescence microscope (Olympus, Tokyo, Japan).

Flow cytometry

5×10^5 C6 cells were seeded at 6-well culture plates and incubated for 24 h. The cells were incubated with 160 μg/mL FA-AuNCs. After 24 h incubation with the FA-AuNCs, the cells were washed 3 times with PBS and then detached by trypsin (Sigma, CA, USA). The flow cytometer (BD FACS Calibur, CA, USA) was employed to evaluate the FA-AuNC incubated cells. The final data were analyzed using FlowJo Software. All samples were performed in triplicate.

Clonogenic cell survival assay

The enhancement of radiation therapy efficacy by the radiosensitizing effect of FA-AuNCs was assessed by clonogenic cell survival assay. The method of calculation was based on previous studies.[16] 10^5 cells were seeded in 35 mm^2 dishes and after 24 h, FA-AuNCs were added and the cells were incubated for another 24 h. Then, cells were irradiated with different doses of X-rays (0, 2, 4, 6, and 8 Gy). The cells were washed with PBS and then, trypsinized to have a single cell suspension. These procedures were done immediately after irradiation. After exact cell counting, the appropriate number of cells was reseeded in triplicates in 100 mm^2 Petri plates for 2-3 weeks at normal cell culture condition. After this time period, methanol was used to fix the cancer cells colonies. Then, crystal violet (0.5%) was used to stain the fixed colonies. The stained colonies were counted by a loupe microscope (Olympus, Tokyo, Japan).[16,17] The survival curves were drawn to obtain the dose enhancement factor (DEF).[10] For more details please refer to our previous publication.[15]

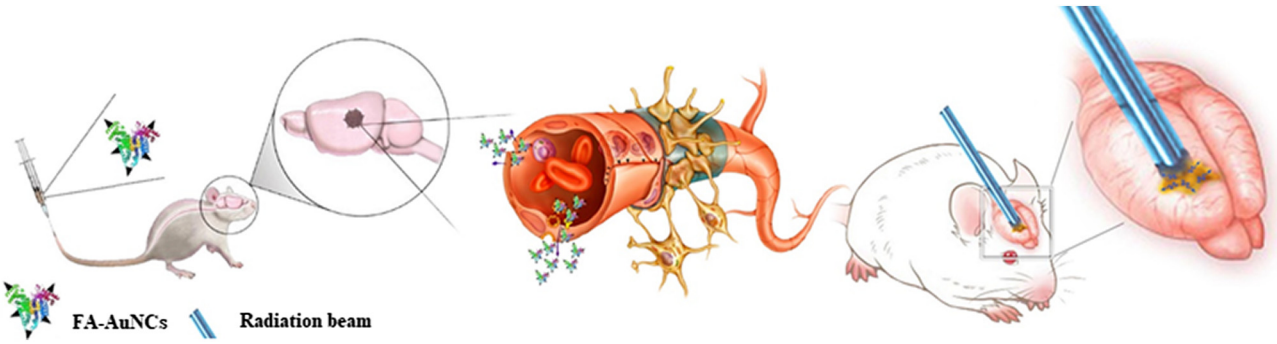

Figure 1. Schematic view of FA-AuNCs mechanism of action for BBB penetration, brain tumor targeting, and enhancement of brain tumors radiation therapy efficacy.

Ethics statement

This study was approved by institutional review committee of Arak University of Medical Sciences and all procedures were reviewed and approved by Institutional Animal Care and Ethics Committee of Arak University of Medical Sciences according to their guidelines for care and use of the laboratory animal.

Intracranial tumor implantation

Female Wistar rats (6-8 weeks old) were purchased from the Pasteur Institute of Tehran, Iran. Rats were obtained for 1 week and maintained at standard conditions: 24 ± 2 °C temperature, 50% ± 10% relative humidity, and 12 h light/12 h dark. All rats were fed sterilized standard chow and water *ad libitum*. The rats were anesthetized by intraperitoneal injection of ketamine/xylazine mixture. Then, rats were immobilized on the stereotactic frame. At first, the cranial skin was cut at the sagittal direction and skin borders were pulled over to reveal cranial bones. A hole was drilled into the skull which was located at 2 mm posterior and 1.5 lateral to the bregma by 0.45 mm burr drill. 1×10^6 C6 cells suspended in Hanks' buffered saline (Sigma, CA, USA) were injected into the burr hole at a depth of 3 mm slowly. The needle was left in place for 3 min and then withdrawn slowly with careful drying of the skull using a microsurgical sponge spear to remove any tumor containing fluid that might reflux out of the burr hole during implantation. Finally, bone wax was applied and skin borders sutured. Survival was calculated from the date of cancer cells implantation and the survival data were plotted using Kaplan–Meier curve.

FA-AuNC biodistribution

For evaluation of the FA-AuNC intracranial distribution, tumor-bearing rats were injected intravenously (i.v) with 10 mg/kg FA-AuNCs after one week from the C6 cells' intracranial implantation. Rats were scarified by an overdose of pentobarbital sodium 24 h after injection and the brain, kidney, liver, spleen, and lung were harvested. 500 mg of these organs, brain tumor, and also, its surrounding normal brain tissue were prepared for measuring gold concentration. The samples were dried at 105 °C until no change at their weights was observed. The products were homogenized in powder and a solution containing 12.5 M hydrochloric acid and 5 M nitric acid was added to each sample. The samples were kept at room temperature until complete dissolving of powdered tissues. The Au concentrations in the tumor and normal brain tissue in this given volume were measured by Inductively Coupled Plasma Optical Emission Spectrometry, ICP-OES (Varian Vista-Pro, Australia).

In vivo radiation therapy

After one week from intracranial implantation of C6 cancer cells, the tumor-bearing rats were divided into four groups (n = 8) including 1) treated with PBS, 2) treated with the FA-AuNCs, 3) treated with radiation alone, and 4) the FA-AuNCs plus radiation therapy. In the first group, tumor-bearing rats were injected with PBS (100 μl per rat). For the second and fourth groups, 10 mg/kg FA-AuNCs were i.v. injected and the fourth group of tumor-bearing rats was irradiated with a single dose of 6 Gy. Also, the third group just was treated with 6 Gy radiation dose. Irradiations were performed using a Compact linear accelerator (Primus, Siemens Ltd., Germany) with a source-surface distance (SSD) of 100 cm and a field size of 20×20 cm^2. To minimize animals' movement through irradiation, they were anesthetized with the combination of ketamine and xylazine.

Histopathology and blood biochemistry exams

For evaluating toxicity of FA-AuNCs, rats were injected with 10 mg/kg FA-AuNCs (n = 3) and sacrificed after 3 days. Their blood was collected and plasma was discarded for alanine transaminase (ALT), aspartate transaminase (AST), blood urea nitrogen (BUN), creatinine (CREA) analyzes. Also, the brain, lung, spleen, kidney, and liver were harvested and fixed in 10% formalin neutral buffer solution and embedded in paraffin for histopathology investigations. In the next step, dehydration was done and samples were blocked. Thin sections about 5 μm were prepared and stained by hematoxylin and eosin. Histological photographs were obtained using a digital light microscope (Olympus, Tokyo, Japan). All the histopathological studies were done by blinded evaluation from a board-certified pathologist.

Immunostaining

The tumor-bearing rats were sacrificed 3 days after radiation therapy (n = 3). The brain tumors (n = 3) from the PBS treated group, treated with radiation alone, and FA-AuNCs plus radiation therapy were harvested and prepared for immunohistochemistry (IHC). Briefly, paraffin-embedded brain tumor tissues were sectioned, deparaffinized, rehydrated, incubated in 3% H_2O_2, and blocked with 5% bovine serum albumin.[18] IHC was conducted with

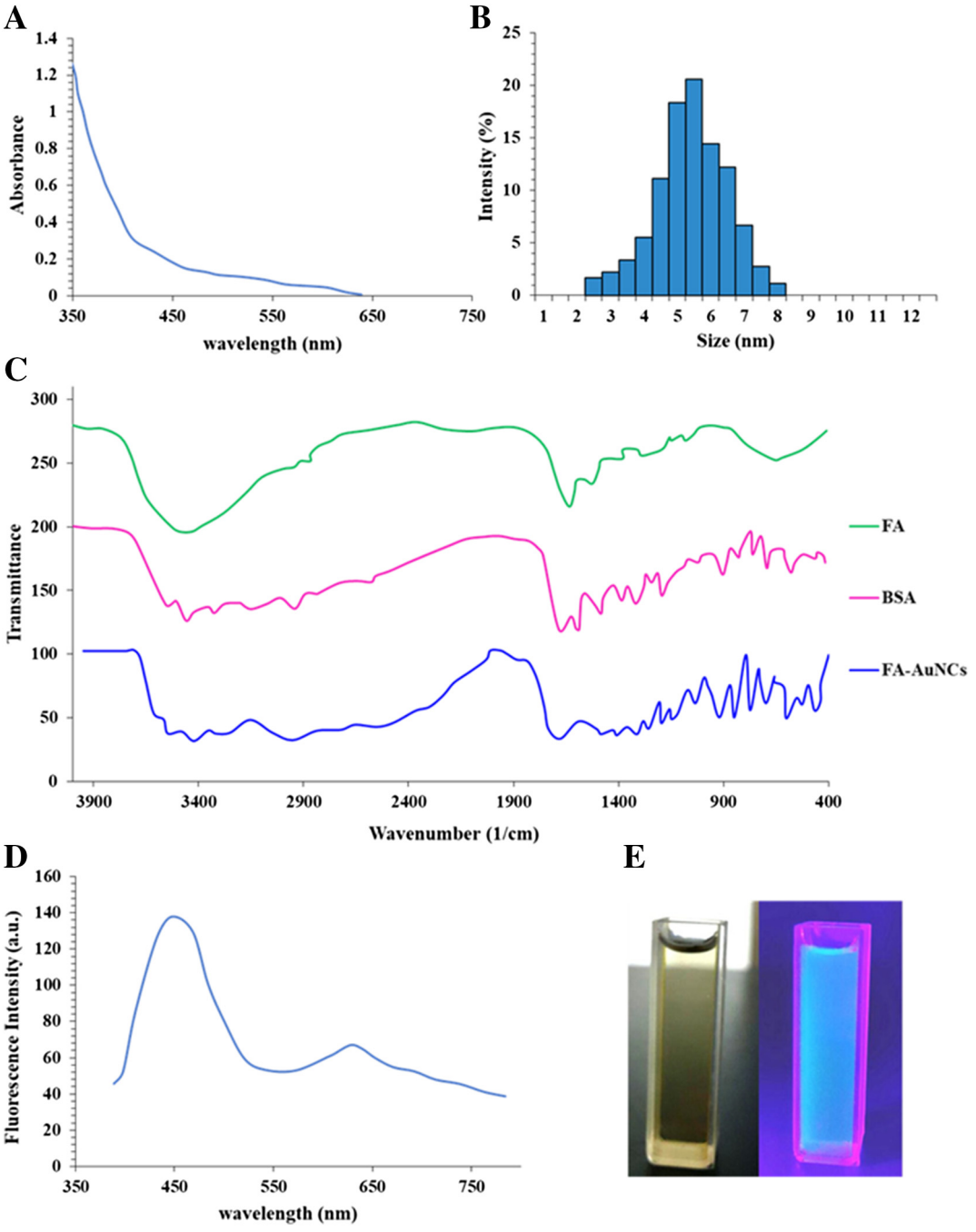

Figure 2. Characterization of the FA-AuNCs. **(A)** UV–Vis absorption spectrum. **(B)** The hydrodynamic size of the FA-AuNCs. **(C)** The FT-IR spectra of BSA, FA, and FA-AuNCs. **(D)** The fluorescence spectrum of the FA-AuNCs. **(E)** Photographs of FA-AuNCs vials under the normal (left) and ultraviolet (right) lamps.

biotinylated rabbit anti-mouse IgG, streptavidin-horseradish peroxidase, 1,3-diaminobenzidine (DAB) tetrahydrochloride, anti-Ki-67 antibody (Abcam, CA, USA), and hematoxylin. Microscopic fields were randomly selected and their images were captured at ×400 magnification. Immuno-positive cells were quantified by a board-certified pathologist at a blinded evaluation. Histological photographs were obtained using a digital light microscope (Olympus, Tokyo, Japan).

Statistical analysis

JMP 11.0 software was employed for performing the statistical analyzes. All data were analyzed by One Way ANOVA and $P < 0.05$ was set as statistical significance. All experiments were repeated at least 3 times and the results were shown as mean ± standard deviation. (*: $P < 0.05$, **: $P < 0.005$, ***: P 0.001, ns: not significant).

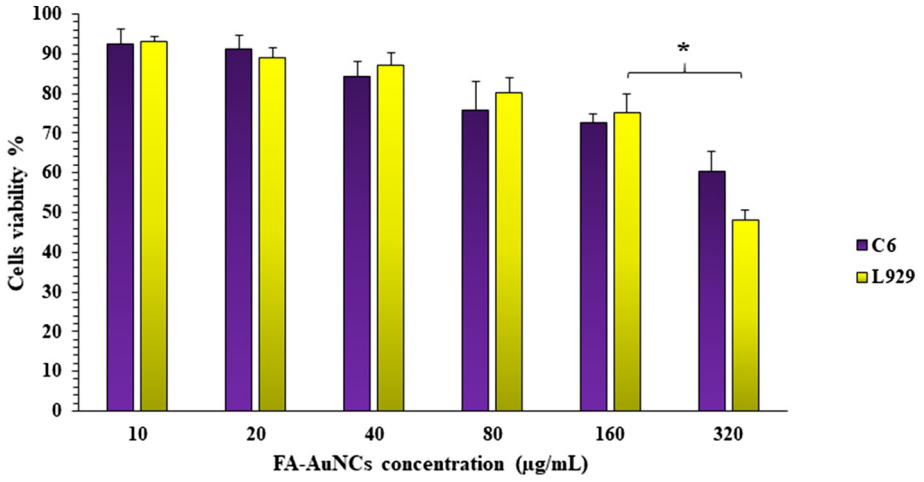

Figure 3. The optimum concentration for using FA-AuNCs *in vitro*. The C6 and L929 cells were incubated for 24 h with different concentrations of FA-AuNCs (10, 20, 40, 80, 160, 320 μg/mL). A significant decrease in the normal cells' viability is apparent at 320 μg/mL concentration of FA-AuNCs (*: $P < 0.05$). For each concentration, 3 wells were evaluated and the experiment was replicated 3 times.

Results

The main purpose of the present study is to utilize FA-AuNCs as brain tumor-specific radiosensitizers for enhancement of radiation therapy efficacy. FA-AuNCs not only can penetrate the BBB but also target the cancer cells in the brain tissue. Efficient accumulation of FA-AuNCs at the malignant cells increases radiation beams' interaction with gold atoms and subsequently, causes more deposition of energy at the tumor. (See Figure 1.)

Characterization of FA-AuNCs

FA-AuNCs exhibit a continuous absorption band without any obvious peak in the UV–Vis absorption spectrum (Figure 2, *A*). The DLS analyses exhibit 5.5 ± 0.4 nm hydrodynamic size and 0.005 polydispersity index for FA-AuNCs (Figure 2, *B*). Figure 2, *C* illustrates the FT-IR spectrum of BSA, FA, and FA-AuNCs. The characteristic amide I band of BSA is apparent at 1683 cm^{-1} as was predictable for a protein with a high proportion of α-helix. The band appearing at 1587.00 cm^{-1} can be attributed to strong primary amine scissoring, whereas the band centered at 3456.98 cm^{-1} can be attributed to primary amines. The 2940.79 cm^{-1} band corresponds to C–H vibration and the broad band at 720.65 cm^{-1} can be attributed to −NH2 and −NH wagging. In FA-AuNCs spectrum, C–H stretching at 2943.00 cm^{-1} and aromatic ring stretch of the pyridine and p-amino benzoic acid moieties in the range of 1300-1700 cm^{-1} which are characteristic vibrational modes associated with FA can be obviously seen. The line broadening appearing over 1700-1300 cm^{-1} is revealing the covalent linkage of FA with BSA.[19] Fluorescence spectrum (Figure 2, *D*) shows a maximum emission at 450 nm with 360 nm excitation wavelength. The photograph of the FA-AuNCs suspension under the ultraviolet lamps is illustrated in Figure 2, *E*.

The optimum concentration of FA-AuNCs for in vitro experiments according to its cellular toxicity

Toxicity is a big challenge in utilizing nanomaterials.[20] Therefore, the highest dose of the FA-AuNCs which had acceptable toxicity for normal cells was selected for further experiments. Also, an ideal concentration of FA-AuNCs should more significantly affect cancer cells than normal cells. The effect of FA-AuNCs' different concentrations on cancer and normal cells' viability was investigated by MTT assay (Figure 3). The increase of the FA-AuNCs' concentrations up to 160 μg/mL exhibited low toxicity for both cell lines (viability percentage > 70%). However, significant toxicity was observed for the normal cells ($P < 0.05$) at 320 μg/mL concentration. Therefore, the 160 μg/mL concentration as the highest dose with appropriate toxicity for the normal cells was utilized for all the further *in vitro* experiments.

FA-AuNCs has significant uptake by the glioma cancer cells in vitro and in vivo

Nanomaterials' effectiveness as radiosensitizer has a direct relationship with their internalization by the target cancer cells. For evaluating FA-AuNC uptake by C6 cancer cells, the cells were incubated with FA-AuNCs (160 μg/mL) for 24 h and their internalization was investigated by fluorescent microscopy and flow cytometry. The FA-AuNCs treated cancer cells exhibited a blue appearance at the fluorescence microscope images as FA-AuNCs emitted blue fluorescent light at the inner of the cancer cells (Figure 4, *E* and *F*). In addition, FA-AuNCs' uptake significantly increased cancer cells' side scatter due to increase of their granularity (Figure 4, *A*, *B*, *C* and Table 1). Also, an increase in the mean fluorescent intensity of the cancer cells was observed due to the fluorescent emission of the internalized FA-AuNCs in comparison with PBS treated C6 cells ($P < 0.05$) (Figure 4, *D*), which is favorable with the fluorescent microscope observations. These observations demonstrate efficient uptake of FA-AuNCs by the glioma cells which can cause a determinative effect on their radiosensitizing efficacy.

For quantitative assessment of FA-AuNCs' uptake by the cancer and normal cells, the C6 and L929 cells were incubated for 6, 12, and 24 h with FA-AuNCs (160 μg/mL). As Figure 5 illustrates, ICP-OES evaluations demonstrated that the cancer cells internalized FA-AuNCs much more than the normal cells,

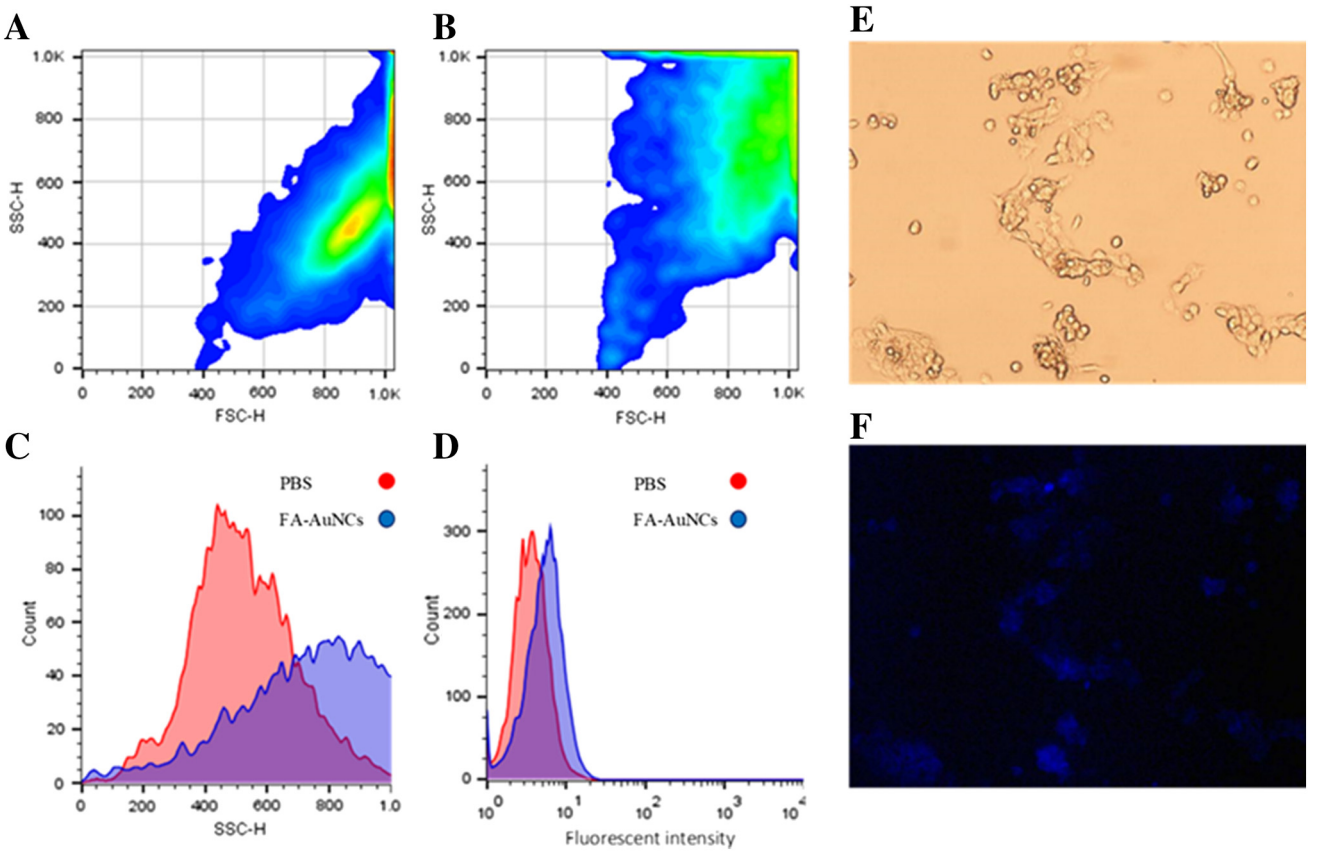

Figure 4. Assessment of FA-AuNC uptake by the cancer cells according to flow cytometry and fluorescent microscopy analyzes. **(A)** The cancer cells' dot plot after incubation with PBS. **(B)** The cancer cells' dot plot after 24 h incubation with FA-AuNCs (160 μg/mL). **(C)** The SSC histogram of the cancer cells with and without incubation with FA-AuNCs (160 μg/mL, 24 h). **(D)** The fluorescent intensity histogram of the cancer cells with and without FA-AuNCs incubation (160 μg/mL, 24 h). The glioma cancer cells exhibited a considerable increase in cellular granularity and fluorescent intensity after 24 h incubation with FA-AuNCs. **(E)** Light microscope photograph of C6 cancer cells 24 h after incubation with FA-AuNCs. **(F)** Fluorescent microscope photograph of the same field. Blue emission of the cancer cell at fluorescent microscope after FA-AuNCs uptake was observed. These observations can strongly demonstrate the efficient uptake of FA-AuNCs by the glioma cancer cells.

Table 1
Evaluation of FA-AuNCs uptake by the cancer cells according to flow cytometry parameters analysis.

Groups	SSC mean	Mean fluorescent intensity
PBS	528 ± 46.1	4.7 ± 0.6
FA-AuNCs	780 ± 93.6*	10.3 ± 2.2*

PBS: phosphate buffer solution, SSC: side scatter.
* $P < 0.05$.

especially after 24 h incubation. Cancer cells exhibited more interest for the FA-AuNCs uptake as they had more intracellular gold content in all the time points in comparison with the normal cells ($P < 0.05$). It should be noticed that the normal cells' gold content increased by time passing, but always cancer cells had higher intracellular gold content ($P < 0.05$). The most intracellular gold content for the cancer cells was detected after 24 h (32.85 ± 4.31) which was significantly ($P < 0.05$) higher than the normal cells' gold content at the same time (13.15 ± 2.75).

The main goal of this study is to conquer the BBB and better gold delivery to intracranial glioma tumors for improvement of radiation therapy efficacy. Therefore, the gold concentration at the intracranial C6 glioma tumors is very determinative which will deeply affect the radiation therapy outcome. The FA-AuNCs (10 mg/kg) were injected intravenously and gold concentration was measured by ICP-OES at the normal brain tissue and tumors 24 h after injection. As Figure 5 illustrates, significantly higher gold concentration was detected at tumoral tissue in comparison with the normal brain tissue. Therefore, FA-AuNCs not only can penetrate the BBB but also target the C6 cancer cells in the brain tissue. Also, FA-AuNCs' toxicity for brain tissue was evaluated by histopathology exams three days after i.v. injection of 10 mg/kg FA-AuNCs (n = 3). There was no sign of brain tissue damage at FA-AuNCs injected rats' brain histopathology (Figure 5, *D* and *E*). Therefore, the FA-AuNCs can be considered safe for brain tissue.

FA-AuNCs significantly enhance radiation therapy efficiency

FA-AuNCs' effect on enhancement of radiation therapy efficacy was investigated by clonogenic cell survival assay. As shown in Figure 6, *A*, a significant enhancement in the radiation therapy efficiency was observed for the FA-AuNCs treated cells

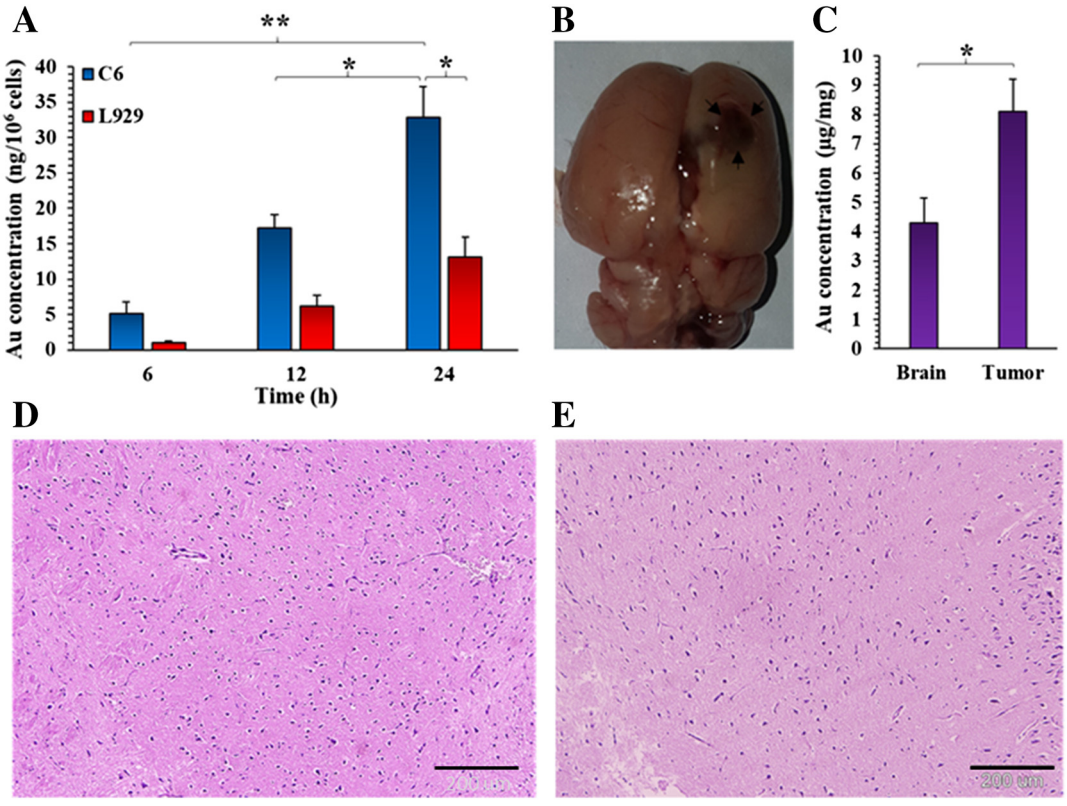

Figure 5. Assessment of FA-AuNCs uptake by the normal and cancer cells *in vitro* and *in vivo*. **(A)** The cancer and normal cells gold content at different time points after FA-AuNCs incubation. ICP-OES exhibited significantly more FA-AuNCs internalization by the C6 cancer cells in comparison with the normal cells, especially after 24 h incubation ($P < 0.05$). **(B)** A C6 brain tumor (indicated by black arrows). **(C)** Intracranial distribution of FA-AuNCs, 24 h after i.v. injection (10 mg/kg). In addition, to evaluate the FA-AuNCs toxicity for brain tissue, normal rats were i.v. injected with 10 mg/kg FA-AuNCs and their brains were harvested 3 days after injection and were stained with H&E (n = 3). **(D)** Control brain tissue histopathology image. **(E)** Brain tissue histopathology photograph 3 days after FA-AuNCs injection.

as the acquired DEF factor for FA-AuNCs was 1.6. This fact can be attributed to efficient FA-AuNC internalization by the glioma cells. The more intracellular gold content of cancer cells enhances more interaction with radiation beams which induces DNA damage and subsequent cancer cells' apoptosis.[21,22]

To have a better simulation of the clinical condition, C6 glioma intracranial tumor animal model and megavoltage radiations as the most common clinical radiation were utilized. This animal model is very similar to human glioblastoma tumors due to its fast proliferation and invasion.[23] C6 cancer cells were implanted into the Wistar rats' brain and the tumor-bearing rats were irradiated 3 days after the tumor implantation. FA-AuNCs were injected (10 mg/kg i.v.) 24 h before radiation therapy. As Figure 6, *B* illustrates, radiation therapy increased tumor-bearing rats' survival about 5 days in comparison with no-treatment group (n = 8, $P < 0.05$). The FA-AuNCs didn't affect the rats' survival *per se*. However, combination of FA-AuNCs as radiosensitizer with radiation therapy caused significant increase ($P < 0.001$, 12 days) in the rats' survival time (Table 2) in comparison with radiation therapy group (n = 8). Therefore, FA-AuNCs not only can impressively target the intracranial tumors but also cause significant enhancement of radiation therapy efficacy.

Ki-67 is a marker which indicates the proliferating cells and quantitatively estimates the tumors' growth, thereby aiding in identifying the prognosis of patients and the treatment efficacy.[24,25] The Ki-67 labeling index was 48.89% ± 9.93% for control group (n = 3), 29.98% ± 8.32% for RT group (n = 3), and 11.53% ± 7.65% for FA-AuNCs + RT (n = 3). Therefore, RT + FA-AuNCs could significantly decrease the Ki-67 index in comparison with no-treatment ($P < 0.001$) and RT ($P < 0.05$) groups. The proliferating cells' number was significantly decreased when the FA-AuNCs were utilized as radiosensitizers and caused enhancement of radiation therapy efficacy (Figure 6, *C, D, E*). These results are consistent with the tumor-bearing rats' survival test in which their main death reason is C6 cancer cell proliferation. Therefore, effective inhibition of cancer cell proliferation in the RT + FA-AuNCs group is the main reason for their survival time increase.

FA-AuNCs' presence at the normal brain tissue doesn't cause toxicity per se and in combination with radiation therapy

Although the brain tumors exhibited high FA-AuNCs content, low concentration of gold nanoclusters was detected at the brain's normal tissue (Figure 5, *C*). Some concerns may rise due to the FA-AuNCs' presence at the brain's normal tissue including long term side effects or increase of radiation damage to the brain. Therefore, to evaluate the effect of FA-AuNCs on the brain, two groups of rats were i.v. injected with 10 mg/kg and

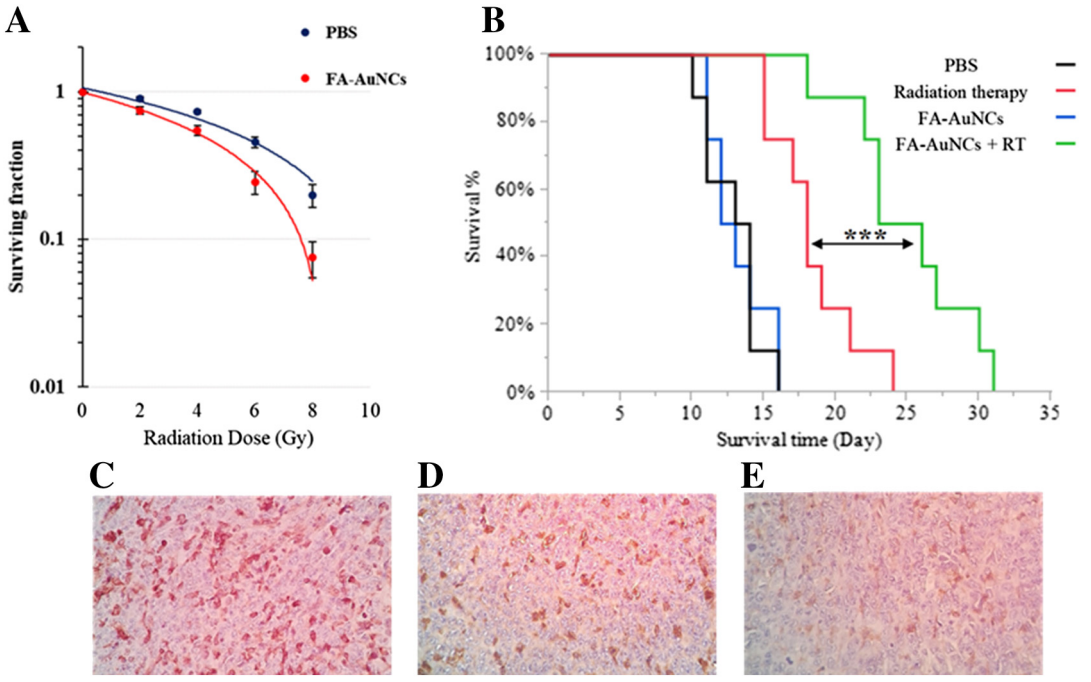

Figure 6. Enhancement of radiation therapy efficacy by utilizing FA-AuNCs at clonogenic survival assay and C6 tumor-bearing rats' treatment. In addition, the brain tumor samples were stained by Ki-67 specific antibody to identify proliferating cells**. (A)** The acquired DEF factor for the FA-AuNCs was 1.6. **(B)** Tumor-bearing rats' survival time in different treatment groups. The FA-AuNCs treatment didn't inhibit tumor growth *per se* as FA-AuNCs had the same survival time as the PBS treated groups. However, FA-AuNCs exhibited significant radiosensitizing effect which was apparent at the difference between the RT and RT + FA-AuNCs treated rats' survival time. **(C)** Immunostained sections of brain tumors of PBS treated group (n = 3). **(D)** RT group (n = 3). **(E)** FA-AuNCs +6 Gy RT treated group (n = 3). All magnifications are ×400.

Table 2
Tumor-bearing rats' survival time at different treatment groups.

Groups	Mean survival time (days)	Median survival time (days)
PBS	12.8 ± 0.7	13.5
FA-AuNCs	13.1 ± 0.7	12.5
RT	18.3 ± 1.0	18
FA-AuNCs + RT	25.0 ± 1.5	24.5

PBS: phosphate buffer solution, RT: radiation therapy.

one of the groups was irradiated with 6 Gy radiation 24 h after the FA-AuNC administration. The rats were observed for 20 days and their weight was monitored. Smallest damages at the brain can cause significant disruption at the rats' behaviors and cause anorexia, weight loss, or even central nerve system dysfunction like ataxia.[26,27] No sign of anorexia, weight loss, cachexia or death was observed (Figure 7). Therefore, presence of FA-AuNCs at the brain tissue does not cause considerable damage even after radiation therapy.

Biodistribution and biocompatibility of FA-AuNCs

FA-AuNCs were i.v. injected (10 mg/kg) to the normal rats (n = 3) and the gold concentration at different organs was investigated after 24 h by ICP-OES. As Figure 8, *A* illustrates, kidney, liver, spleen, and lung exhibited approximately the same gold content ($P > 0.05$). Accumulation of the nanomaterials at the vital organs may cause toxicity. Therefore, rats (n = 3) were i.v. injected with FA-AuNCs (10 mg/kg) and sacrificed after 3 days to investigate the FA-AuNCs effect by blood biochemistry (Figure 8, *B*) and histopathology (Figure 8, *C*) exams. No sign of liver and kidney function test disruption was observed. In addition, the histopathological evaluations exhibited no toxicity for vital organs. It is obvious that intravenous injection of FA-AuNCs is completely safe and has no toxicity for the body organs.

Discussion

RT is the most common therapeutic approach for brain tumors. However, brain tumors' radioresistance can significantly decrease the RT outcomes.[28] Although different radiosensitizers have been utilized for the enhancement of RT efficacy, brain tumors' sensitizing to the radiation therapy has a big obstacle which is the inability to deliver radiosensitizers to the brain due to BBB. Overcoming this challenge is very determinative in improving brain tumors' RT efficacy.[29] In addition, efficient targeting of malignant cells in the brain tissue can significantly enhance the therapeutic efficacy of RT and decrease the side effects.[6,30]

GNPs have been synthesized with a vast variety of decorations and characterizations. They are well-known radiosensitizers because of their high atomic number which causes a more efficient interaction with radiation beams.[2] However, the sufficient uptake and internalization of GNPs by cancer cells are the most determinative parameters for radiosensitizing efficacy.[31] This fact becomes more prominent in the brain tumors in which their

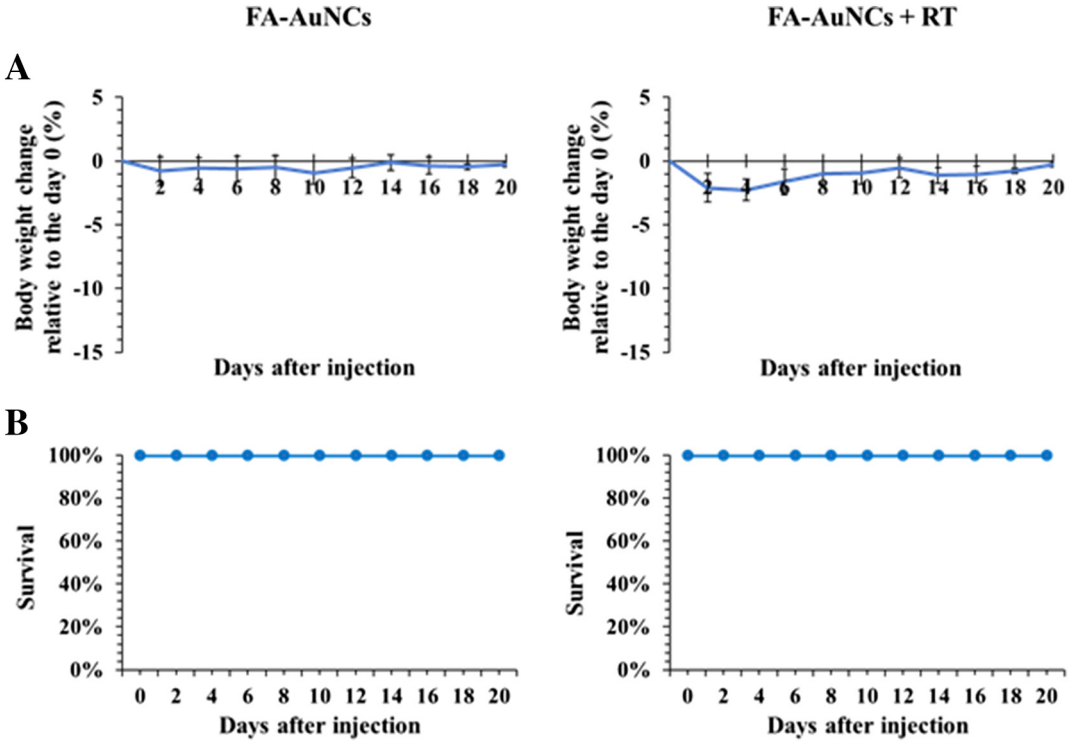

Figure 7. Assessment of FA-AuNCs effect on normal brain tissue *per se* and in combination with radiation therapy. Two groups of rats were i.v. injected with 10 mg/kg. One of the groups was irradiated with 6 Gy radiation, 24 h after FA-AuNCs administration. **(A)** No sign of weight loss or **(B)** death was observed in both groups (n = 5).

decoration should have the ability to cross the BBB. Subsequently, more accumulation of GNPs at the tumoral tissue by efficient targeting of cancer cells can significantly enhance radiation therapy efficacy.[32,33]

The BBB consists of brain capillary endothelial cells and their tight junctions are adhering them together. Its main function is to act as a selective barrier which separates the brain from circulating toxins and potentially harmful chemicals and allowing access to a small subset of molecules with the appropriate properties.[34–36] Hence, more than 98% of small molecular drugs and almost all large molecules are barred from the brain tissues.[37] Three major mechanisms are involved in the penetration of nanoparticles through BBB including passive diffusion, endocytosis, and carrier-mediated transport.[29,38] These mechanisms can be employed in various modalities to enhance internalization of nanomaterials into the brain. Several studies have improved brain tumors' targeting by decorating nanoparticles with ligands that are substrates for BBB transporters.[12,38–40] Receptor-mediated transport can enter large molecules and some vitamins into the brain. Our designed radiosensitizer is self-targeting with folic acid (FA). FA is a low MW vitamin (441 Da) and one of the most promising ligands that have been used as a tumor-targeting agent.[41] Folate receptors are highly overexpressed on the surface of a wide variety of human carcinomas; head and neck, breast, ovary, kidney, lung, and brain.[42–45] But, distribution of this receptor in the normal tissue is extremely restricted.[40,46] Also, many studies have demonstrated the expression of folate receptors on the luminal side of BBB endothelial cells which can facilitate the transit of FA decorated nanomaterials through BBB.[47] Therefore, in this study, FA was selected as the targeting decoration of nanoclusters for more efficient transfer from the BBB and brain tumor specific-targeting.

Modification of GNPs with organic materials such as bovine serum albumin (BSA) can cause enhanced permeation retention (EPR) effect and subsequently increase the nanoparticles' accumulation in tumors.[15,48] BSA protein acts as a stable capping agent in synthesis of ultra-small GNPs[46,49] with uniform size and stability under physiological conditions.[50] In addition, BSA is a promising cap for nanoclusters formation. The metal core of gold nanoclusters has significantly higher surface to volume ratio in comparison with other gold nanostructures including nanoparticles, nanostars, and nanorods due to the unique gold atoms' arrangement.[51] This fact is very determinative in metal radiosensitizers' efficacy as the interaction of radiation beams with gold atoms' surface causes high energy deposition and consequent damage of cancer cells. Therefore, the gold nanoclusters may be the most appropriate form of gold nanostructures for radiosensitizing purposes and enhancement of radiation therapy efficacy. However, extremely rare studies have focused on their radiosensitizing ability.[52]

The size of the nanoparticles, as well as their surface decoration, can affect their ability to cross BBB. The accumulation of GNPs in the tumor is size-dependent. Several studies demonstrated the effect of nanoparticles size on their tumor targeting ability.[53,54] In addition, smaller GNPs were able to penetrate deeply into tumor rather than larger GNPs.[55] Decreasing the nanoparticle size can enhance the delivery efficiency in tumor

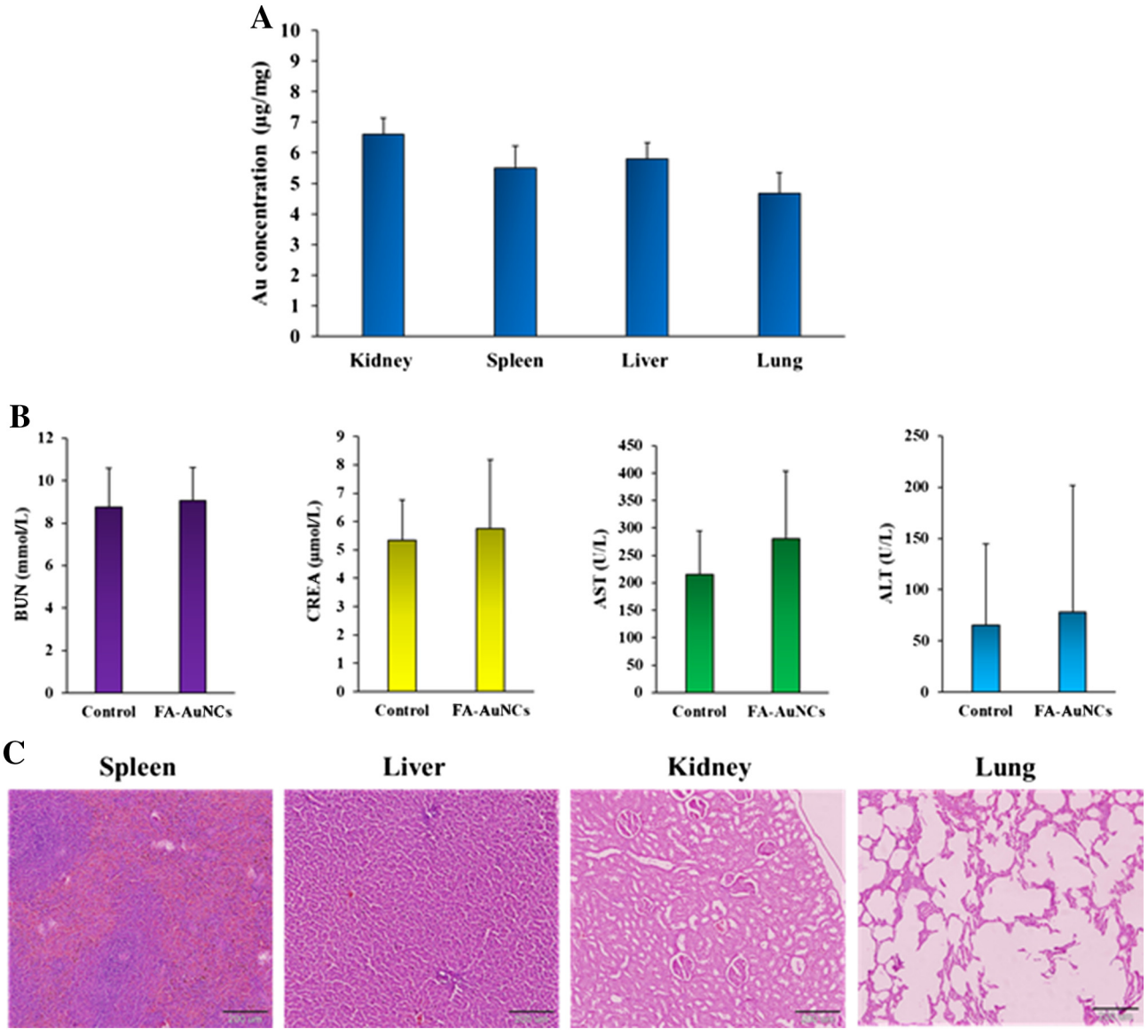

Figure 8. Biodistribution and biocompatibility of FA-AuNCs. **(A)** Biodistribution of FA-AuNCs (n = 3), 24 h after i.v. administration (10 mg/kg). **(B)** Blood biochemical exams of rats (n = 3) for liver and kidney function, 3 days after FA-AuNCs i.v. injection (10 mg/kg). **(C)** Images of H&E stained tissue sections from spleen, liver, kidney, and lung of rats (n = 3), 3 days after FA-AuNCs i.v. injection (10 mg/kg).

tissue and improve the radiation therapy efficacy.[56,57] In addition, it was reported that smaller GNPs (2 and 6 nm) were distributed in the cytoplasm and nucleus of cancer cells, while larger GNPs (15 nm) were located only in the cytoplasm.[57] Therefore, the smaller GNPs can reach the main action site of radiation which means nucleus and cancer cells' DNA. Gold nanoclusters had exhibited many advantages over other gold nanostructures due to their ultra-small size including significant tumor targeting efficacy,[58] intratumoral penetration,[57] efficient renal clearance to prevent unwanted organs accumulation,[59] evading from RES trapping[60] and subsequently, more tumor accumulation.

Overall, folic acid targeted and BSA capped AuNCs were applied as targeted radiosensitizers for improving brain tumor radiation therapy efficacy. To have more translatable results for clinical usage, routine clinical MV radiation dose and one of the most similar animal brain tumor models to human glioblastoma were utilized. The ultra-small FA-AuNCs with biocompatible and stable bovine serum albumin copping were designed and were conjugated with folic acid for more effective BBB crossing and intracranial cancer cells' targeting. This complex system had significant targeting efficacy for intracranial glioma tumors and undeniable effect on increase of brain tumor-bearing rats' survival time.

References

1. Krex D, Klink B, Hartmann C, von Deimling A, Pietsch T, Simon M, et al. Long-term survival with glioblastoma multiforme. *Brain* 2007;**130**:2596-606.
2. Rosa S, Connolly C, Schettino G, Butterworth KT, Prise KM. Biological mechanisms of gold nanoparticle radiosensitization. *Cancer Nanotechnol* 2017;**8**:2.

3. Koul D, Shen R, Bergh S, Sheng X, Shishodia S, Lafortune TA, et al. Inhibition of Akt survival pathway by a small-molecule inhibitor in human glioblastoma. *Mol Cancer Ther* 2006;**5**:637-44.
4. Mi Y, Shao Z, Vang J, Kaidar-Person O, Wang AZ. Application of nanotechnology to cancer radiotherapy. *Cancer Nanotechnol* 2016;**7**:11.
5. Dong X. Current strategies for brain drug delivery. *Theranostics* 2018;**8**:1481.
6. Joh DY, Sun L, Stangl M, Al Zaki A, Murty S, Santoiemma PP, et al. Selective targeting of brain tumors with gold nanoparticle-induced radiosensitization. *PLoS One* 2013;**8**e62425.
7. Lee C-F, You P-Y, Lin Y-C, Hsu T-L, Cheng P-Y, Wu Y-X, et al. Exploring the stability of gold nanoparticles by experimenting with adsorption interactions of nanomaterials in an undergraduate lab. *J Chem Educ* 2015;**92**:1066-70.
8. Orlando A, Colombo M, Prosperi D, Corsi F, Panariti A, Rivolta I, et al. Evaluation of gold nanoparticles biocompatibility: a multiparametric study on cultured endothelial cells and macrophages. *J Nanopart Res* 2016;**18**:58.
9. Hainfeld JF, Smilowitz HM, O'connor MJ, Dilmanian FA, Slatkin DN. Gold nanoparticle imaging and radiotherapy of brain tumors in mice. *Nanomedicine* 2013;**8**:1601-9.
10. Rahman WN, Bishara N, Ackerly T, He CF, Jackson P, Wong C, et al. Enhancement of radiation effects by gold nanoparticles for superficial radiation therapy. *Nanomedicine* 2009;**5**:136-42.
11. Cloughesy TF, Black KL. Pharmacological blood-brain barrier modification for selective drug delivery. *J Neurooncol* 1995;**26**:125-32.
12. Shilo M, Sharon A, Baranes K, Motiei M, Lellouche J-PM, Popovtzer R. The effect of nanoparticle size on the probability to cross the blood-brain barrier: an in-vitro endothelial cell model. *J Nanobiotechnol* 2015;**13**:19.
13. Bourassa P, Hasni I, Tajmir-Riahi H. Folic acid complexes with human and bovine serum albumins. *Food Chem* 2011;**129**:1148-55.
14. Cundall R. *Time-resolved fluorescence spectroscopy in biochemistry and biology*. Springer Science & Business Media; 2013.
15. Ghahremani F, Shahbazi-Gahrouei D, Kefayat A, Motaghi H, Mehrgardi MA, Javanmard SH. AS1411 aptamer conjugated gold nanoclusters as a targeted radiosensitizer for megavoltage radiation therapy of 4T1 breast cancer cells. *RSC Adv* 2018;**8**:4249-58.
16. Franken NA, Rodermond HM, Stap J, Haveman J, Van Bree C. Clonogenic assay of cells in vitro. *Nat Protoc* 2006;**1**:2315-9.
17. Munshi A, Hobbs M, Meyn RE. Clonogenic cell survival assay. *Chemosensitivity: Volume 1 In Vitro Assays*; 2005. p. 21-8.
18. Rose DP, Connolly JM. *Influence of dietary fat intake on local recurrence and progression of metastases arising from MDA-MB-435 human breast cancer cells in nude mice after excision of the primary tumor*; 1992.
19. Xavier PL, Chaudhari K, Verma PK, Pal SK, Pradeep T. Luminescent quantum clusters of gold in transferrin family protein, lactoferrin exhibiting FRET. *Nanoscale* 2010;**2**:2769-76.
20. Ray PC, Yu H, Fu PP. Toxicity and environmental risks of nanomaterials: challenges and future needs. *J Environ Sci Health C* 2009;**27**:1-35.
21. Chithrani DB, Jelveh S, Jalali F, van Prooijen M, Allen C, Bristow RG, et al. Gold nanoparticles as radiation sensitizers in cancer therapy. *Radiat Res* 2010;**173**:719-28.
22. Marques T, Chatterjee D, Nicolucci P, Krishnan S. Enhanced radiosensitization by tumor-targeting gold nanoparticles: a paradigm for energy modulated radiation therapy (EMRT). *Radiat Oncol Biol Phys* 2013;**87**:S658.
23. Grobben B, De Deyn P, Slegers H. Rat C6 glioma as experimental model system for the study of glioblastoma growth and invasion. *Cell Tissue Res* 2002;**310**:257-70.
24. Tseng Y-Y, Su C-H, Yang S-T, Huang Y-C, Lee W-H, Wang Y-C, et al. Advanced interstitial chemotherapy combined with targeted treatment of malignant glioma in rats by using drug-loaded nanofibrous membranes. *Oncotarget* 2016;759902.
25. Kim EJ, Choi M-R, Park H, Kim M, Hong JE, Lee J-Y, et al. Dietary fat increases solid tumor growth and metastasis of 4T1 murine mammary carcinoma cells and mortality in obesity-resistant BALB/c mice. *Breast Cancer Res* 2011;**13**:R78.
26. Hazarika RJJoe b. Neurotoxic impact of organophosphate pesticide phosphomedon on the albino rat. 2014;**35**:427.
27. Yuan Z-Y, Hu Y-L, Gao J-QJPo. Brain localization and neurotoxicity evaluation of polysorbate 80-modified chitosan nanoparticles in rats. 2015;**10**e0134722.
28. Kelley K, Knisely J, Symons M, Ruggieri R. Radioresistance of brain tumors. *Cancer* 2016;**8**:42.
29. Oberoi RK, Parrish KE, Sio TT, Mittapalli RK, Elmquist WF, Sarkaria JN. Strategies to improve delivery of anticancer drugs across the blood–brain barrier to treat glioblastoma. *Neuro Oncol* 2015;**18**:27-36.
30. Patel RR, Mehta MP. Targeted therapy for brain metastases: improving the therapeutic ratio. *Clin Cancer Res* 2007;**13**:1675-83.
31. Ngwa W, Kumar R, Sridhar S, Korideck H, Zygmanski P, Cormack RA, et al. Targeted radiotherapy with gold nanoparticles: current status and future perspectives. *Nanomedicine* 2014;**9**:1063-82.
32. Lee J, Chatterjee DK, Lee MH, Krishnan S. Gold nanoparticles in breast cancer treatment: promise and potential pitfalls. *Cancer Lett* 2014;**347**:46-53.
33. Mieszawska AJ, Mulder WJ, Fayad ZA, Cormode DP. Multifunctional gold nanoparticles for diagnosis and therapy of disease. *Mol Pharm* 2013;**10**:831-47.
34. Van Tellingen O, Yetkin-Arik B, De Gooijer M, Wesseling P, Wurdinger T, De Vries H. Overcoming the blood–brain tumor barrier for effective glioblastoma treatment. *Drug Resist Updat* 2015;**19**:1-12.
35. Abbott NJ, Rönnbäck L, Hansson E. Astrocyte–endothelial interactions at the blood–brain barrier. *Nat Rev Neurosci* 2006;**7**:41.
36. Aryal M, Vykhodtseva N, Zhang Y-Z, McDannold N. Multiple sessions of liposomal doxorubicin delivery via focused ultrasound mediated blood–brain barrier disruption: a safety study. *J Control Release* 2015;**204**:60-9.
37. Pardridge WM. Blood–brain barrier endogenous transporters as therapeutic targets: a new model for small molecule CNS drug discovery. *Expert Opin Ther Targets* 2015;**19**:1059-72.
38. Wang S, Meng Y, Li C, Qian M, Huang R. Receptor-mediated drug delivery systems targeting to glioma. *Nanomaterials* 2015;**6**:3.
39. Shilo M, Motiei M, Hana P, Popovtzer R. Transport of nanoparticles through the blood–brain barrier for imaging and therapeutic applications. *Nanoscale* 2014;**6**:2146-52.
40. Niu J, Wang A, Ke Z, Zheng Z. Glucose transporter and folic acid receptor-mediated pluronic P105 polymeric micelles loaded with doxorubicin for brain tumor treating. *J Drug Target* 2014;**22**:712-23.
41. Zwicke GL, Ali Mansoori G, Jeffery CJ. Utilizing the folate receptor for active targeting of cancer nanotherapeutics. *Nano Rev* 2012;**3**18496.
42. Parker N, Turk MJ, Westrick E, Lewis JD, Low PS, Leamon CP. Folate receptor expression in carcinomas and normal tissues determined by a quantitative radioligand binding assay. *Anal Biochem* 2005;**338**:284-93.
43. Zhao X, Li H, Lee RJ. Targeted drug delivery via folate receptors. *Expert Opin Drug Deliv* 2008;**5**:309-19.
44. O'Shannessy DJ, Yu G, Smale R, Fu Y-S, Singhal S, Thiel RP, et al. Folate receptor alpha expression in lung cancer: diagnostic and prognostic significance. *Oncotarget* 2012;**3**:414.
45. O'Shannessy DJ, Somers EB, Maltzman J, Smale R, Fu Y-S. Folate receptor alpha (FRA) expression in breast cancer: identification of a new molecular subtype and association with triple negative disease. *Springerplus* 2012;**1**:22.
46. Liang S, Jin X, Ma Y, Guo J, Wang H. Folic acid-conjugated BSA nanocapsule (n-BSA–FA) for cancer targeted radiotherapy and imaging. *RSC Adv* 2015;**5**:88560-6.
47. Chen Y-C, Chiang C-F, Chen L-F, Liang P-C, Hsieh W-Y, Lin W-L. Polymersomes conjugated with des-octanoyl ghrelin and folate as a BBB-penetrating cancer cell-targeting delivery system. *Biomaterials* 2014;**35**:4066-81.
48. Chen N, Yang W, Bao Y, Xu H, Qin S, Tu Y. BSA capped Au nanoparticle as an efficient sensitizer for glioblastoma tumor radiation therapy. *RSC Adv* 2015;**5**:40514-20.

49. AL-Jawad SM, Taha AA, Al-Halbosiy MM, AL-Barram LF. Synthesis and characterization of small-sized gold nanoparticles coated by bovine serum albumin (BSA) for cancer photothermal therapy. *Photodiagnosis Photodyn Ther* 2018;**21**:201-10.
50. Zhang X-D, Wu D, Shen X, Liu P-X, Fan F-Y, Fan S-J. In vivo renal clearance, biodistribution, toxicity of gold nanoclusters. *Biomaterials* 2012;**33**:4628-38.
51. Sokolowska K. *Surface modification of gold nanoparticles and nanoclusters*; 2016.
52. Zhang X-D, Luo Z, Chen J, Song S, Yuan X, Shen X, et al. Ultrasmall glutathione-protected gold nanoclusters as next generation radiotherapy sensitizers with high tumor uptake and high renal clearance. *Sci Rep* 2015;**5**:8669.
53. Arvizo R, Bhattacharya R, Mukherjee P. Gold nanoparticles: opportunities and challenges in nanomedicine. *Expert Opin Drug Deliv* 2010;**7**:753-63.
54. Chithrani BD, Ghazani AA, Chan WC. Determining the size and shape dependence of gold nanoparticle uptake into mammalian cells. *Nano Lett* 2006;**6**:662-8.
55. Wang J, Mao W, Lock LL, Tang J, Sui M, Sun W, et al. The role of micelle size in tumor accumulation, penetration, and treatment. *ACS Nano* 2015;**9**:7195-206.
56. Kim B, Han G, Toley BJ, Kim C-k, Rotello VM, Forbes NS. Tuning payload delivery in tumour cylindroids using gold nanoparticles. *Nat Nanotechnol* 2010;**5**:465.
57. Huang K, Ma H, Liu J, Huo S, Kumar A, Wei T, et al. Size-dependent localization and penetration of ultrasmall gold nanoparticles in cancer cells, multicellular spheroids, and tumors in vivo. *ACS Nano* 2012;**6**:4483-93.
58. Dreaden EC, Austin LA, Mackey MA, El-Sayed MA. Size matters: gold nanoparticles in targeted cancer drug delivery. *Ther Deliv* 2012;**3**:457-78.
59. Longmire M, Choyke PL, Kobayashi H. *Clearance properties of nano-sized particles and molecules as imaging agents: considerations and caveats*; 2008.
60. Guo S, Huang L. Nanoparticles escaping RES and endosome: challenges for siRNA delivery for cancer therapy. *J Nanomater* 2011;**2011**:11.